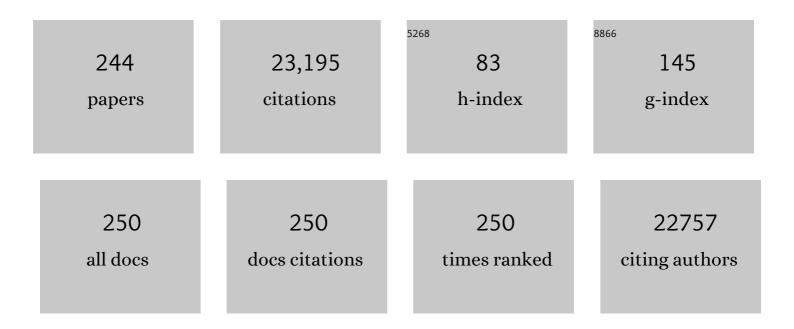
Jae Sung Lee

List of Publications by Year in descending order

Source: https://exaly.com/author-pdf/685531/publications.pdf Version: 2024-02-01



INE SUNCLEE

#	Article	IF	CITATIONS
1	Self-motivated, thermally oxidized hematite nanoflake photoanodes: Effects of pre-polishing and ZrO2 passivation layer. Journal of Energy Chemistry, 2022, 65, 415-423.	12.9	11
2	Sulfurâ€doped molybdenum phosphide as fast dis/charging anode for Liâ€ion and Naâ€ion batteries. International Journal of Energy Research, 2022, 46, 8452-8463.	4.5	7
3	Metal substrates activate NiFe(oxy)hydroxide catalysts for efficient oxygen evolution reaction in alkaline media. Journal of Alloys and Compounds, 2022, 901, 163689.	5.5	16
4	An <i>in situ</i> fluorine and <i>ex situ</i> titanium two-step co-doping strategy for efficient solar water splitting by hematite photoanodes. Nanoscale Advances, 2022, 4, 1659-1667.	4.6	9
5	Photoelectrochemical Nitrate Reduction to Ammonia on Ordered Silicon Nanowire Array Photocathodes. Angewandte Chemie, 2022, 134, .	2.0	2
6	Photoelectrochemical Nitrate Reduction to Ammonia on Ordered Silicon Nanowire Array Photocathodes. Angewandte Chemie - International Edition, 2022, 61, .	13.8	25
7	Microwave-assisted metal-ion attachment for ex-situ zirconium doping into hematite for enhanced photoelectrochemical water splitting. Renewable Energy, 2022, 189, 694-703.	8.9	17
8	Hetero-tandem organic solar cells drive water electrolysis with a solar-to-hydrogen conversion efficiency up to 10%. Applied Catalysis B: Environmental, 2022, 309, 121237.	20.2	8
9	Highly Efficient Photoelectrochemical Hydrogen Production Using Nontoxic Culn _{1.5} Se ₃ Quantum Dots with ZnS/SiO ₂ Double Overlayers. ACS Applied Materials & Interfaces, 2022, 14, 603-610.	8.0	7
10	Healing Ion-Implanted Semiconductors by Hybrid Microwave Annealing: Activation of Nitrogen-Implanted TiO ₂ . Journal of Physical Chemistry Letters, 2022, 13, 3878-3885.	4.6	1
11	Molecularly Engineered Carbon Platform To Anchor Edge-Hosted Single-Atomic M–N/C (M = Fe, Co, Ni,) Tj ETÇ	0q1_1_0.78 11.2	4314 rgBT /○
12	Design of 2D Layered Catalyst by Coherent Heteroepitaxial Conversion for Robust Hydrogen Generation. Advanced Functional Materials, 2021, 31, 2005449.	14.9	11
13	Nanostructured Iron Sulfide/N, S Dual-Doped Carbon Nanotube-Graphene Composites as Efficient Electrocatalysts for Oxygen Reduction Reaction. Materials, 2021, 14, 2146.	2.9	19
14	Base-free CO2 hydrogenation to formic acid over Pd supported on defective carbon nitride modified by microwave and acid treatments. Journal of Catalysis, 2021, 396, 395-401.	6.2	17
15	Metal carbides as alternative electrocatalysts for energy conversion reactions. Journal of Catalysis, 2021, 404, 911-924.	6.2	20
16	Layered Double Hydroxide-Derived Intermetallic Ni ₃ GaC _{0.25} Catalysts for Dry Reforming of Methane. ACS Catalysis, 2021, 11, 11091-11102.	11.2	26
17	Rational design of photocatalysts for ammonia production from water and nitrogen gas. Nano Convergence, 2021, 8, 22.	12.1	18
18	Innovative strategies toward challenges in PV-powered electrochemical CO2 reduction. Journal of Energy Chemistry, 2021, 60, 410-416.	12.9	23

#	Article	IF	CITATIONS
19	ZnFe ₂ O ₄ Dendrite/SnO ₂ Helix 3D Hetero‣tructure Photoanodes for Enhanced Photoelectrochemical Water Splitting: Triple Functions of SnO ₂ Nanohelix. Small, 2021, 17, e2103861.	10.0	14
20	A Brief History of Nuclear Medicine Physics, Instrumentation, and Data Sciences in Korea. Nuclear Medicine and Molecular Imaging, 2021, 55, 265-284.	1.0	0
21	Intentional Extrinsic Doping into ZnFe 2 O 4 Nanorod Photoanode for Enhanced Photoelectrochemical Water Splitting. Solar Rrl, 2020, 4, 1900328.	5.8	13
22	Nitrogen-doped carbon nanotube–graphene hybrid stabilizes MxN (M = Fe, Co) nanoparticles for efficient oxygen reduction reaction. Applied Catalysis B: Environmental, 2020, 268, 118415.	20.2	46
23	Covalent 0D–2D Heterostructuring of Co ₉ S ₈ –MoS ₂ for Enhanced Hydrogen Evolution in All pH Electrolytes. Advanced Functional Materials, 2020, 30, 2002536.	14.9	114
24	Gradient tantalum-doped hematite homojunction photoanode improves both photocurrents and turn-on voltage for solar water splitting. Nature Communications, 2020, 11, 4622.	12.8	133
25	Immobilizing single atom catalytic sites onto highly reduced carbon hosts: Fe–N ₄ /CNT as a durable oxygen reduction catalyst for Na–air batteries. Journal of Materials Chemistry A, 2020, 8, 18891-18902.	10.3	31
26	Recycling Carbon Dioxide through Catalytic Hydrogenation: Recent Key Developments and Perspectives. ACS Catalysis, 2020, 10, 11318-11345.	11.2	215
27	Cobalt Ferrite Nanoparticles to Form a Catalytic Co–Fe Alloy Carbide Phase for Selective CO ₂ Hydrogenation to Light Olefins. ACS Catalysis, 2020, 10, 8660-8671.	11.2	95
28	Nanostructured molybdenum Phosphide/N-Doped carbon nanotube-graphene composites as efficient electrocatalysts for hydrogen evolution reaction. Applied Catalysis A: General, 2020, 594, 117451.	4.3	20
29	Structure-tunable supraparticle assemblies of hollow cupric oxide sheathed with nanographenes. Nanoscale Advances, 2020, 2, 1236-1244.	4.6	5
30	Ferrites: emerging light absorbers for solar water splitting. Journal of Materials Chemistry A, 2020, 8, 9447-9482.	10.3	61
31	Immiscible bi-metal single-atoms driven synthesis of electrocatalysts having superb mass-activity and durability. Applied Catalysis B: Environmental, 2020, 270, 118896.	20.2	102
32	Benchmark performance of low-cost Sb2Se3 photocathodes for unassisted solar overall water splitting. Nature Communications, 2020, 11, 861.	12.8	135
33	Seawater-Mediated Solar-to-Sodium Conversion by Bismuth Vanadate Photoanode- Photovoltaic Tandem Cell: Solar Rechargeable Seawater Battery. IScience, 2019, 19, 232-243.	4.1	16
34	Hybrid Microwave Annealing Synthesizes Highly Crystalline Nanostructures for (Photo)electrocatalytic Water Splitting. Accounts of Chemical Research, 2019, 52, 3132-3142.	15.6	27
35	A Few Atomic FeNbO ₄ Overlayers on Hematite Nanorods: Microwave-Induced High Temperature Phase for Efficient Photoelectrochemical Water Splitting. ACS Catalysis, 2019, 9, 1289-1297.	11.2	58
36	Precipitating Metal Nitrate Deposition of Amorphous Metal Oxyhydroxide Electrodes Containing Ni, Fe, and Co for Electrocatalytic Water Oxidation. ACS Catalysis, 2019, 9, 9650-9662.	11.2	43

Jae Sung Lee

#	Article	IF	CITATIONS
37	Three Birds, Oneâ€Stone Strategy for Hybrid Microwave Synthesis of Ta and Sn Codoped Fe ₂ O ₃ @FeTaO ₄ Nanorods for Photoâ€Electrochemical Water Oxidation. Advanced Functional Materials, 2019, 29, 1805737.	14.9	79
38	Multi-atlas cardiac PET segmentation. Physica Medica, 2019, 58, 32-39.	0.7	9
39	Band Gap Narrowing of Zinc Orthogermanate by Dimensional and Defect Modification. Journal of Physical Chemistry C, 2019, 123, 14573-14581.	3.1	6
40	Precisely-controlled, a few layers of iron titanate inverse opal structure for enhanced photoelectrochemical water splitting. Nano Energy, 2019, 62, 20-29.	16.0	24
41	Solar Water Splitting: Elaborately Modified BiVO ₄ Photoanodes for Solar Water Splitting (Adv. Mater. 20/2019). Advanced Materials, 2019, 31, 1970146.	21.0	64
42	Toward practical solar hydrogen production – an artificial photosynthetic leaf-to-farm challenge. Chemical Society Reviews, 2019, 48, 1908-1971.	38.1	781
43	Elaborately Modified BiVO ₄ Photoanodes for Solar Water Splitting. Advanced Materials, 2019, 31, e1806938.	21.0	333
44	Electrocatalytic property of water oxidation reaction depends on charging state of intermediates on Ag-M (M = Fe, co, Ni, Cu) in alkaline media. International Journal of Hydrogen Energy, 2019, 44, 5863-5871.	7.1	5
45	Reduced perovskite LaNiO3 catalysts modified with Co and Mn for low coke formation in dry reforming of methane. Applied Catalysis A: General, 2019, 575, 198-203.	4.3	107
46	Activating the surface and bulk of hematite photoanodes to improve solar water splitting. Chemical Science, 2019, 10, 10436-10444.	7.4	57
47	Perovskite Tandems Advance Solar Hydrogen Production. Joule, 2019, 3, 2892-2894.	24.0	7
48	Key Strategies to Advance the Photoelectrochemical Water Splitting Performance of αâ€Fe ₂ O ₃ Photoanode. ChemCatChem, 2019, 11, 157-179.	3.7	135
49	Activating MoS ₂ Basal Plane with Ni ₂ P Nanoparticles for Ptâ€Like Hydrogen Evolution Reaction in Acidic Media. Advanced Functional Materials, 2019, 29, 1809151.	14.9	114
50	Photoelectrochemical Water Splitting with pâ€īype Metal Oxide Semiconductor Photocathodes. ChemSusChem, 2019, 12, 1835-1845.	6.8	96
51	Exfoliated NiFe Layered Double Hydroxide Cocatalyst for Enhanced Photoelectrochemical Water Oxidation with Hematite Photoanode. ChemCatChem, 2019, 11, 443-448.	3.7	22
52	Hybrid Microwave Annealing for Fabrication of More Efficient Semiconductor Photoanodes for Solar Water Splitting. ACS Sustainable Chemistry and Engineering, 2019, 7, 944-949.	6.7	15
53	Efficient Hydrogen Evolution Reaction Catalysis in Alkaline Media by Allâ€inâ€One MoS ₂ with Multifunctional Active Sites. Advanced Materials, 2018, 30, e1707105.	21.0	321
54	Metalâ€Free Artificial Photosynthesis of Carbon Monoxide Using Nâ€Doped ZnTe Nanorod Photocathode Decorated with Nâ€Doped Carbon Electrocatalyst Layer. Advanced Energy Materials, 2018, 8, 1702636.	19.5	42

#	Article	IF	CITATIONS
55	Ultrapermeable Nickel–Cobalt–Manganese/Alumina Inverse Opal as a Cokeâ€∓olerant and Pressureâ€Dropâ€Free Catalyst for the Dry Reforming of Methane. ChemCatChem, 2018, 10, 2214-2218.	3.7	12
56	Highly loaded PbS/Mn-doped CdS quantum dots for dual application in solar-to-electrical and solar-to-chemical energy conversion. Applied Catalysis B: Environmental, 2018, 227, 409-417.	20.2	59
57	One-dimensional CuIn alloy nanowires as a robust and efficient electrocatalyst for selective CO2-to-CO conversion. Journal of Power Sources, 2018, 378, 412-417.	7.8	35
58	Effective charge separation in site-isolated Pt-nanodot deposited PbTiO3 nanotube arrays for enhanced photoelectrochemical water splitting. Applied Catalysis B: Environmental, 2018, 224, 804-809.	20.2	34
59	A precious metal-free solar water splitting cell with a bifunctional cobalt phosphide electrocatalyst and doubly promoted bismuth vanadate photoanode. Journal of Materials Chemistry A, 2018, 6, 1266-1274.	10.3	51
60	Hydrogen Evolution Reaction: Encapsulating Iridium Nanoparticles Inside a 3D Cageâ€Like Organic Network as an Efficient and Durable Catalyst for the Hydrogen Evolution Reaction (Adv. Mater.) Tj ETQqO 0 0 rgE	3T þ æ rlo	ck 10 Tf 50 5
61	Sulfur-Doped Dicobalt Phosphide Outperforming Precious Metals as a Bifunctional Electrocatalyst for Alkaline Water Electrolysis. Chemistry of Materials, 2018, 30, 8861-8870.	6.7	71
62	Encapsulating Iridium Nanoparticles Inside a 3D Cage‣ike Organic Network as an Efficient and Durable Catalyst for the Hydrogen Evolution Reaction. Advanced Materials, 2018, 30, e1805606.	21.0	98
63	All-Bismuth-Based Oxide Tandem Cell for Solar Overall Water Splitting. ACS Applied Energy Materials, 2018, 1, 6694-6699.	5.1	22
64	Bifunctional sulfur-doped cobalt phosphide electrocatalyst outperforms all-noble-metal electrocatalysts in alkaline electrolyzer for overall water splitting. Nano Energy, 2018, 53, 286-295.	16.0	184
65	Boosting the performance of Cu2O photocathodes for unassisted solar water splitting devices. Nature Catalysis, 2018, 1, 412-420.	34.4	489
66	Boron- and Nitrogen-Codoped Molybdenum Carbide Nanoparticles Imbedded in a BCN Network as a Bifunctional Electrocatalyst for Hydrogen and Oxygen Evolution Reactions. ACS Catalysis, 2018, 8, 8296-8305.	11.2	126
67	A multitude of modifications strategy of ZnFe2O4 nanorod photoanodes for enhanced photoelectrochemical water splitting activity. Journal of Materials Chemistry A, 2018, 6, 12693-12700.	10.3	52
68	Density Functional Theory (DFT) Calculations for Oxygen Reduction Reaction Mechanisms on Metal-, Nitrogen- co-doped Graphene (M-N2-G (M = Ti, Cu, Mo, Nb and Ru)) Electrocatalysts. Electrochimica Acta, 2017, 228, 619-627.	5.2	29
69	2D materials-based photoelectrochemical cells: Combination of transition metal dichalcogenides and reduced graphene oxide for efficient charge transfer. FlatChem, 2017, 4, 54-60.	5.6	18
70	Autoâ€Reduction Behavior of Cobalt on Graphitic Carbon Nitride Coated Alumina Supports for Fischer–Tropsch Synthesis. ChemCatChem, 2017, 9, 4098-4104.	3.7	18
71	Effect of lattice strain on nanomaterials in energy applications: A perspective on experiment and theory. International Journal of Hydrogen Energy, 2017, 42, 16064-16107.	7.1	12
72	BCN network-encapsulated multiple phases of molybdenum carbide for efficient hydrogen evolution reactions in acidic and alkaline media. Journal of Materials Chemistry A, 2017, 5, 13122-13129.	10.3	82

#	Article	IF	CITATIONS
73	Sulfur and Nitrogen Dual-Doped Molybdenum Phosphide Nanocrystallites as an Active and Stable Hydrogen Evolution Reaction Electrocatalyst in Acidic and Alkaline Media. ACS Catalysis, 2017, 7, 3030-3038.	11.2	210
74	Screening of Oxygen-Reduction-Reaction-Efficient Electrocatalysts Based on Ag–M (M = 3d, 4d, and 5d) Tj ET 1874-1881.	Qq0 0 0 rg 5.1	BT /Overlock 13
75	Freeze-dried MoS ₂ sponge electrodes for enhanced electrochemical energy storage. Dalton Transactions, 2017, 46, 2122-2128.	3.3	67
76	Sodium ontaining Spinel Zinc Ferrite as a Catalyst Precursor for the Selective Synthesis of Liquid Hydrocarbon Fuels. ChemSusChem, 2017, 10, 4764-4770.	6.8	89
77	Water Splitting: Engineering Highly Ordered Iron Titanate Nanotube Array Photoanodes for Enhanced Solar Water Splitting Activity (Adv. Funct. Mater. 35/2017). Advanced Functional Materials, 2017, 27, .	14.9	7
78	Current progress and scientific challenges in the advancement of organic–inorganic lead halide perovskite solar cells. New Journal of Chemistry, 2017, 41, 10508-10527.	2.8	21
79	Engineering Highly Ordered Iron Titanate Nanotube Array Photoanodes for Enhanced Solar Water Splitting Activity. Advanced Functional Materials, 2017, 27, 1702428.	14.9	52
80	Nanomaterials for photocatalytic hydrogen production: from theoretical perspectives. RSC Advances, 2017, 7, 34875-34885.	3.6	51
81	Vertically Aligned Core–Shell PbTiO ₃ @TiO ₂ Heterojunction Nanotube Array for Photoelectrochemical and Photocatalytic Applications. Journal of Physical Chemistry C, 2017, 121, 15063-15070.	3.1	39
82	Carbon dioxide Fischer-Tropsch synthesis: A new path to carbon-neutral fuels. Applied Catalysis B: Environmental, 2017, 202, 605-610.	20.2	230
83	Unbiased Sunlight-Driven Artificial Photosynthesis of Carbon Monoxide from CO ₂ Using a ZnTe-Based Photocathode and a Perovskite Solar Cell in Tandem. ACS Nano, 2016, 10, 6980-6987.	14.6	128
84	A multi-stacked hyperporous silicon flake for highly active solar hydrogen production. Chemical Communications, 2016, 52, 10221-10224.	4.1	21
85	Hetero-type dual photoanodes for unbiased solar water splitting with extended light harvesting. Nature Communications, 2016, 7, 13380.	12.8	263
86	Overall Photoelectrochemical Water Splitting using Tandem Cell under Simulated Sunlight. ChemSusChem, 2016, 9, 61-66.	6.8	112
87	All-in-one synthesis of mesoporous silicon nanosheets from natural clay and their applicability to hydrogen evolution. NPG Asia Materials, 2016, 8, e248-e248.	7.9	56
88	Amorphous MoS _x thin-film-coated carbon fiber paper as a 3D electrode for long cycle life symmetric supercapacitors. Nanoscale, 2016, 8, 11787-11791.	5.6	66
89	Coke tolerance of Ni/Al ₂ O ₃ nanosheet catalyst for dry reforming of methane. Catalysis Science and Technology, 2016, 6, 2060-2064.	4.1	47
90	Enhanced activity of carbon-supported PdCo electrocatalysts toward electrooxidation of ethanol in alkaline electrolytes. Korean Journal of Chemical Engineering, 2016, 33, 1799-1804.	2.7	13

#	Article	IF	CITATIONS
91	Highly Active and Cokeâ€Tolerant Hierarchical Mordenite Catalysts Synthesized by Recrystallization for the Isopropylation of Naphthalene. ChemCatChem, 2016, 8, 2996-3001.	3.7	4
92	Photocatalytic activity of electron-deficient and porous WO3 nanoparticles derived from thermal oxidation of bulk WC particles. Journal of Photochemistry and Photobiology A: Chemistry, 2016, 330, 37-43.	3.9	3
93	Highly Conformal Deposition of an Ultrathin FeOOH Layer on a Hematite Nanostructure for Efficient Solar Water Splitting. Angewandte Chemie - International Edition, 2016, 55, 10854-10858.	13.8	200
94	Highly Conformal Deposition of an Ultrathin FeOOH Layer on a Hematite Nanostructure for Efficient Solar Water Splitting. Angewandte Chemie, 2016, 128, 11012-11016.	2.0	32
95	Oxygen-Intercalated CuFeO ₂ Photocathode Fabricated by Hybrid Microwave Annealing for Efficient Solar Hydrogen Production. Chemistry of Materials, 2016, 28, 6054-6061.	6.7	113
96	Ultrafast fabrication of highly active BiVO ₄ photoanodes by hybrid microwave annealing for unbiased solar water splitting. Nanoscale, 2016, 8, 17623-17631.	5.6	40
97	A highly active and stable palladium catalyst on a g-C ₃ N ₄ support for direct formic acid synthesis under neutral conditions. Chemical Communications, 2016, 52, 14302-14305.	4.1	60
98	Structure engineering of a core/shell Si@Ta3N5 heterojunction nanowires array for photoelectrochemical water oxidation. RSC Advances, 2016, 6, 104955-104961.	3.6	5
99	Hydrogen-doped Brookite TiO2 Nanobullets Array as a Novel Photoanode for Efficient Solar Water Splitting. Scientific Reports, 2016, 6, 36099.	3.3	33
100	Facile surfactant driven fabrication of transparent WO3 photoanodes for improved photoelectrochemical properties. Applied Catalysis A: General, 2016, 521, 233-239.	4.3	10
101	Two-dimensional metal-dielectric hybrid-structured film with titanium oxide for enhanced visible light absorption and photo-catalytic application. Nano Energy, 2016, 21, 115-122.	16.0	21
102	Solar Hydrogen Production from Zinc Telluride Photocathode Modified with Carbon and Molybdenum Sulfide. ACS Applied Materials & Interfaces, 2016, 8, 7748-7755.	8.0	37
103	Photoelectrochemical, impedance and optical data for self Sn-diffusion doped Fe 2 O 3 photoanodes fabricated at high temperature by one and two-step annealing methods. Data in Brief, 2015, 5, 796-804.	1.0	16
104	Tungsten Carbide and CNT–Grapheneâ€Supported Pd Electrocatalyst toward Electrooxidation of Hydrogen. ChemCatChem, 2015, 7, 1483-1489.	3.7	7
105	Selective Formation of HÃǥg Iron Carbide with g ₃ N ₄ as a Sacrificial Support for Highly Active Fischer–Tropsch Synthesis. ChemCatChem, 2015, 7, 3488-3494.	3.7	46
106	Influence of Metal Particle Size on Oxidative CO ₂ Reforming of Methane over Supported Nickel Catalysts: Effects of Secondâ€Metal Addition. ChemCatChem, 2015, 7, 1445-1452.	3.7	24
107	MOR/SBAâ€15 Composite Catalysts with Interconnected Meso/Micropores for Improved Activity and Stability in Isopropylation of Naphthalene. ChemCatChem, 2015, 7, 2354-2360.	3.7	7
108	Tree branch-shaped cupric oxide for highly effective photoelectrochemical water reduction. Nanoscale, 2015, 7, 7624-7631.	5.6	90

#	Article	IF	CITATIONS
109	Nanostructure-Preserved Hematite Thin Film for Efficient Solar Water Splitting. ACS Applied Materials & Interfaces, 2015, 7, 14123-14129.	8.0	69
110	Carbonate-coordinated cobalt co-catalyzed BiVO4/WO3 composite photoanode tailored for CO2 reduction to fuels. Nano Energy, 2015, 15, 153-163.	16.0	113
111	Catalytic CO ₂ hydrogenation to formic acid over carbon nanotube-graphene supported PdNi alloy catalysts. RSC Advances, 2015, 5, 105560-105566.	3.6	99
112	Bifunctional TiO ₂ underlayer for α-Fe ₂ O ₃ nanorod based photoelectrochemical cells: enhanced interface and Ti ⁴⁺ doping. Journal of Materials Chemistry A, 2015, 3, 5007-5013.	10.3	90
113	Fine-Tuning Pulse Reverse Electrodeposition for Enhanced Photoelectrochemical Water Oxidation Performance of î±-Fe ₂ O ₃ Photoanodes. Journal of Physical Chemistry C, 2015, 119, 5281-5292.	3.1	30
114	Ultrafast synthesis of MoS2 or WS2-reduced graphene oxide composites via hybrid microwave annealing for anode materials of lithium ion batteries. Journal of Power Sources, 2015, 295, 228-234.	7.8	82
115	One-pot synthesis of NiFe layered double hydroxide/reduced graphene oxide composite as an efficient electrocatalyst for electrochemical and photoelectrochemical water oxidation. Journal of Power Sources, 2015, 294, 437-443.	7.8	183
116	Recent theoretical progress in the development of photoanode materials for solar water splitting photoelectrochemical cells. Journal of Materials Chemistry A, 2015, 3, 10632-10659.	10.3	146
117	Phase transition-induced band edge engineering of BiVO ₄ to split pure water under visible light. Proceedings of the National Academy of Sciences of the United States of America, 2015, 112, 13774-13778.	7.1	116
118	Defective ZnFe ₂ O ₄ nanorods with oxygen vacancy for photoelectrochemical water splitting. Nanoscale, 2015, 7, 19144-19151.	5.6	183
119	Wireless Solar Water Splitting Device with Robust Cobalt-Catalyzed, Dual-Doped BiVO ₄ Photoanode and Perovskite Solar Cell in Tandem: A Dual Absorber Artificial Leaf. ACS Nano, 2015, 9, 11820-11829.	14.6	219
120	One-Pot Defunctionalization of Lignin-Derived Compounds by Dual-Functional Pd ₅₀ Ag ₅₀ /Fe ₃ O ₄ /N-rGO Catalyst. ACS Catalysis, 2015, 5, 6964-6972.	11.2	62
121	Selective CO production by Au coupled ZnTe/ZnO in the photoelectrochemical CO ₂ reduction system. Energy and Environmental Science, 2015, 8, 3597-3604.	30.8	152
122	Awakening Solar Water‧plitting Activity of ZnFe ₂ O ₄ Nanorods by Hybrid Microwave Annealing. Advanced Energy Materials, 2015, 5, 1401933.	19.5	95
123	BiVO ₄ -Based Heterostructured Photocatalysts for Solar Water Splitting: A Review. Energy and Environment Focus, 2014, 3, 339-353.	0.3	96
124	Photochemistry: A Stable and Efficient Hematite Photoanode in a Neutral Electrolyte for Solar Water Splitting: Towards Stability Engineering (Adv. Energy Mater. 13/2014). Advanced Energy Materials, 2014, 4, n/a-n/a.	19.5	3
125	CaFe2O4 sensitized hierarchical TiO2 photo composite for hydrogen production under solar light irradiation. Chemical Engineering Journal, 2014, 247, 152-160.	12.7	73
126	An exceptionally facile method to produce layered double hydroxides on a conducting substrate and their application for solar water splitting without an external bias. Energy and Environmental Science, 2014, 7, 2301.	30.8	37

#	Article	IF	CITATIONS
127	Aqueousâ€Solution Route to Zinc Telluride Films for Application to CO ₂ Reduction. Angewandte Chemie - International Edition, 2014, 53, 5852-5857.	13.8	91
128	Research Update: Strategies for efficient photoelectrochemical water splitting using metal oxide photoanodes. APL Materials, 2014, 2, .	5.1	120
129	A Stable and Efficient Hematite Photoanode in a Neutral Electrolyte for Solar Water Splitting: Towards Stability Engineering. Advanced Energy Materials, 2014, 4, 1400476.	19.5	110
130	Highly Active and Stable Hydrogen Evolution Electrocatalysts Based on Molybdenum Compounds on Carbon Nanotube–Graphene Hybrid Support. ACS Nano, 2014, 8, 5164-5173.	14.6	531
131	Isopropylation of naphthalene by isopropanol over conventional and Zn- and Fe-modified USY zeolites. Catalysis Science and Technology, 2014, 4, 120-128.	4.1	21
132	Moâ€Compound/CNTâ€Graphene Composites as Efficient Catalytic Electrodes for Quantumâ€Dotâ€Sensitized Solar Cells. Advanced Energy Materials, 2014, 4, 1300775.	19.5	84
133	Palladium oxide as a novel oxygen evolution catalyst on BiVO4 photoanode for photoelectrochemical water splitting. Journal of Catalysis, 2014, 317, 126-134.	6.2	65
134	Improved Photoelectrochemical Activity of CaFe ₂ O ₄ /BiVO ₄ Heterojunction Photoanode by Reduced Surface Recombination in Solar Water Oxidation. ACS Applied Materials & Interfaces, 2014, 6, 17762-17769.	8.0	114
135	A versatile photoanode-driven photoelectrochemical system for conversion of CO2 to fuels with high faradaic efficiencies at low bias potentials. Journal of Materials Chemistry A, 2014, 2, 2044.	10.3	85
136	Fabrication of graphene-based electrode in less than a minute through hybrid microwave annealing. Scientific Reports, 2014, 4, 5492.	3.3	76
137	A highly efficient transition metal nitride-based electrocatalyst for oxygen reduction reaction: TiN on a CNT–graphene hybrid support. Journal of Materials Chemistry A, 2013, 1, 8007.	10.3	126
138	Single-crystalline, wormlike hematite photoanodes for efficient solar water splitting. Scientific Reports, 2013, 3, 2681.	3.3	580
139	Anionâ€Đoped Mixed Metal Oxide Nanostructures Derived from Layered Double Hydroxide as Visible Light Photocatalysts. Advanced Functional Materials, 2013, 23, 2348-2356.	14.9	86
140	TiN Nanoparticles on CNT–Graphene Hybrid Support as Nobleâ€Metalâ€Free Counter Electrode for Quantumâ€Dotâ€Sensitized Solar Cells. ChemSusChem, 2013, 6, 261-267.	6.8	51
141	Photocatalytic selective oxidation of the terminal methyl group of dodecane with molecular oxygen over atomically dispersed Ti in a mesoporous SiO2 matrix. Green Chemistry, 2013, 15, 3387.	9.0	10
142	Inverse opal structured α-Fe2O3 on graphene thin films: enhanced photo-assisted water splitting. Nanoscale, 2013, 5, 1939.	5.6	70
143	Improved activity and coke resistance by promoters of nanosized trimetallic catalysts for autothermal carbon dioxide reforming of methane. Applied Catalysis A: General, 2013, 450, 63-72.	4.3	46
144	Fabrication of CaFe ₂ O ₄ /TaON Heterojunction Photoanode for Photoelectrochemical Water Oxidation. Journal of the American Chemical Society, 2013, 135, 5375-5383.	13.7	282

Jae Sung Lee

#	Article	IF	CITATIONS
145	Barium Substituted Lanthanum Manganite Perovskite for CO ₂ Reforming of Methane. ACS Catalysis, 2013, 3, 1537-1544.	11.2	121
146	Highly Efficient and Stable Cadmium Chalcogenide Quantum Dot/ZnO Nanowires for Photoelectrochemical Hydrogen Generation. Chemistry of Materials, 2013, 25, 184-189.	6.7	106
147	A method for synthesizing ZnO–carbonaceous species nanocomposites, and their conversion to quasi-single crystal mesoporous ZnO nanostructures. RSC Advances, 2012, 2, 566-572.	3.6	8
148	Photocatalytic and Photoelectrochemical Water Oxidation over Metalâ€Đoped Monoclinic BiVO ₄ Photoanodes. ChemSusChem, 2012, 5, 1926-1934.	6.8	311
149	Ti-dopant-enhanced photocatalytic activity of a CaFe2O4/MgFe2O4 bulk heterojunction under visible-light irradiation. Journal of the Korean Physical Society, 2012, 61, 73-79.	0.7	14
150	Photoelectrochemical water splitting over ordered honeycomb hematite electrodes stabilized by alumina shielding. Energy and Environmental Science, 2012, 5, 6375-6382.	30.8	86
151	High Electrochemical Performance and Stability of Co-Deposited Pd–Au on Phase-Pure Tungsten Carbide for Hydrogen Oxidation. Topics in Catalysis, 2012, 55, 922-930.	2.8	24
152	Graphene–carbon nanotube composite as an effective conducting scaffold to enhance the photoelectrochemical water oxidation activity of a hematite film. RSC Advances, 2012, 2, 9415.	3.6	88
153	Light-Induced Cleaning of CdS and ZnS Nanoparticles: Superiority to Annealing as a Postsynthetic Treatment of Functional Nanoparticles. Journal of Physical Chemistry C, 2012, 116, 15427-15431.	3.1	3
154	Phosphate Doping into Monoclinic BiVO ₄ for Enhanced Photoelectrochemical Water Oxidation Activity. Angewandte Chemie - International Edition, 2012, 51, 3147-3151.	13.8	435
155	Formation of Hierarchical Pore Structures in Zn/ZSMâ€5 to Improve the Catalyst Stability in the Aromatization of Branched Olefins. ChemCatChem, 2012, 4, 1143-1153.	3.7	39
156	Imaging of activated cortical areas after light and electrical stimulation of the rabbit retina: F-18 FDG PET-guided brain mapping. Biomedical Engineering Letters, 2012, 2, 111-117.	4.1	5
157	Heterojunction semiconductors: A strategy to develop efficient photocatalytic materials for visible light water splitting. Catalysis Today, 2012, 185, 270-277.	4.4	277
158	Sulfonated resorcinol-formaldehyde polymer gels synthesized in Nafion ion clusters as nanoscale reactors for a filler of hybrid proton exchange membranes. International Journal of Hydrogen Energy, 2012, 37, 9766-9774.	7.1	9
159	Photoelectrochemical Water Splitting for Solar Hydrogen Production over Semiconductor Nanostructures. Rapid Communication in Photoscience, 2012, 1, 39-39.	0.1	Ο
160	Heterojunction BiVO4/WO3 electrodes for enhanced photoactivity of water oxidation. Energy and Environmental Science, 2011, 4, 1781.	30.8	1,068
161	Fabrication of nanoporous MTiO3 (M = Pb, Ba, Sr) perovskite array films with unprecedented high structural regularity. CrystEngComm, 2011, 13, 7212.	2.6	11
162	Sulfur-Emission-Free Process of Molybdenum Carbide Synthesis by Lime-Enhanced Molybdenum Disulfide Reduction with Methane. Industrial & Engineering Chemistry Research, 2011, 50, 13340-13346.	3.7	10

#	Article	IF	CITATIONS
163	Palladium–nickel alloys loaded on tungsten carbide as platinum-free anode electrocatalysts for polymer electrolyte membrane fuel cells. Chemical Communications, 2011, 47, 5792.	4.1	62
164	Solution-based fabrication of ZnO/ZnSe heterostructure nanowire arrays for solar energy conversion. Journal of Materials Chemistry, 2011, 21, 17816.	6.7	40
165	Charge transfer in iron oxide photoanode modified with carbon nanotubes for photoelectrochemical water oxidation: An electrochemical impedance study. International Journal of Hydrogen Energy, 2011, 36, 9462-9468.	7.1	62
166	Engineered Nanorod Perovskite Film Photocatalysts to Harvest Visible Light. Advanced Materials, 2011, 23, 2088-2092.	21.0	57
167	A composite electrolyte membrane containing high-content sulfonated carbon spheres for proton exchange membrane fuel cells. Carbon, 2011, 49, 1367-1373.	10.3	20
168	Enhanced Photocatalytic Properties due to Electron-rich Ti-ion Doping in ZnFe2O4 under Visible Light Irradiation. Journal of the Korean Physical Society, 2011, 59, 2750-2755.	0.7	7
169	Platinum-free tungsten carbides as an efficient counter electrode for dye sensitized solar cells. Chemical Communications, 2010, 46, 8600.	4.1	215
170	Direct synthesis of sulfonated mesoporous silica as inorganic fillers of proton-conducting organic–inorganic composite membranes. Journal of Membrane Science, 2010, 357, 199-205.	8.2	52
171	Nanocrystalline WO3 film with high photo-electrochemical activity prepared by polymer-assisted direct deposition. Scripta Materialia, 2010, 63, 757-760.	5.2	31
172	Cross-modal and compensatory plasticity in adult deafened cats: A longitudinal PET study. Brain Research, 2010, 1354, 85-90.	2.2	16
173	New sulfonic acid moiety grafted on montmorillonite as filler of organic–inorganic composite membrane for non-humidified proton-exchange membrane fuel cells. Journal of Power Sources, 2010, 195, 4653-4659.	7.8	61
174	Nitrogen-doped titanium oxide microrods decorated with titanium oxide nanosheets for visible light photocatalysis. Journal of Materials Research, 2010, 25, 1096-1104.	2.6	3
175	Carbon-doped ZnO nanostructures synthesized using vitamin C for visible light photocatalysis. CrystEngComm, 2010, 12, 3929.	2.6	175
176	The fabrication of highly uniform ZnO/CdS core/shell structures using a spin-coating-based successive ion layer adsorption and reaction method. Nanotechnology, 2010, 21, 325604.	2.6	38
177	Synthesis of hexagonal WO ₃ nanowires by microwave-assisted hydrothermal method and their electrocatalytic activities for hydrogen evolution reaction. Journal of Materials Chemistry, 2010, 20, 1683-1690.	6.7	253
178	Fabrication of a Vertically Aligned Ferroelectric Perovskite Nanowire Array on Conducting Substrate. Chemistry of Materials, 2010, 22, 4806-4813.	6.7	37
179	Controlled Gd2O3 nanorods and nanotubes by the annealing of Gd(OH)3 nanorod and nanotube precursors and self-templates produced by a microwave-assisted hydrothermal process. CrystEngComm, 2010, 12, 2962.	2.6	40
180	Ruthenium atalyzed, Oneâ€Pot Alcohol Oxidation–Wittig Reaction Producing α,βâ€Unsaturated Esters. European Journal of Organic Chemistry, 2009, 2009, 2943-2946.	2.4	53

#	Article	IF	CITATIONS
181	Size effects of WO3 nanocrystals for photooxidation of water in particulate suspension and photoelectrochemical film systems. International Journal of Hydrogen Energy, 2009, 34, 3234-3242.	7.1	218
182	Photocatalytic overall water splitting with dual-bed system under visible light irradiation. International Journal of Hydrogen Energy, 2009, 34, 3243-3249.	7.1	51
183	Heterojunction photocatalyst TiO2/AgGaS2 for hydrogen production from water under visible light. Chemical Physics Letters, 2009, 475, 78-81.	2.6	28
184	Fabrication of CaFe2O4/MgFe2O4 bulk heterojunction for enhanced visible light photocatalysis. Chemical Communications, 2009, , 5889.	4.1	220
185	Fabrication of ZnO/CdS core/shell nanowire arrays for efficient solar energy conversion. Journal of Materials Chemistry, 2009, 19, 5945.	6.7	393
186	Transition Metal Carbides and Nitrides as Electrode Materials for Low Temperature Fuel Cells. Energies, 2009, 2, 873-899.	3.1	372
187	Transesterification of Dimethylcarbonate and Phenol Over Silica Supported TiO2 and Ti-MCM 41 Catalysts: Structure Insensitivity. Catalysis Letters, 2008, 123, 115-122.	2.6	9
188	Assessment of Cerebral Glucose Metabolism in Cat Deafness Model: Strategies for Improving the Voxel-Based Statistical Analysis for Animal PET Studies. Molecular Imaging and Biology, 2008, 10, 154-161.	2.6	22
189	Pt/WC as an anode catalyst for PEMFC: Activity and CO tolerance. Catalysis Today, 2008, 132, 117-122.	4.4	92
190	Role of platinum-like tungsten carbide as cocatalyst of CdS photocatalyst for hydrogen production under visible light irradiation. Applied Catalysis A: General, 2008, 346, 149-154.	4.3	115
191	Location and State of Pt in Platinized CdS/TiO ₂ Photocatalysts for Hydrogen Production from Water under Visible Light. Journal of Physical Chemistry C, 2008, 112, 17200-17205.	3.1	188
192	Phase and photoelectrochemical behavior of solution-processed Fe2O3 nanocrystals for oxidation of water under solar light. Applied Physics Letters, 2008, 93, .	3.3	56
193	Dopant dependent band gap tailoring of hydrothermally prepared cubic SrTixM1â^'xO3 (M=Ru,Rh,Ir,Pt,Pd) nanoparticles as visible light photocatalysts. Applied Physics Letters, 2008, 92, 104107.	3.3	66
194	Solvothermal Synthesis of CdS Nanowires for Photocatalytic Hydrogen and Electricity Production. Journal of Physical Chemistry C, 2007, 111, 13280-13287.	3.1	400
195	Nanoporous Pt/WC as an Anode for Direct Methanol Fuel Cells. Studies in Surface Science and Catalysis, 2007, , 61-66.	1.5	1
196	Rhodium and Iridium Nanoparticles Entrapped in Aluminum Oxyhydroxide Nanofibers: Catalysts for Hydrogenations of Arenes and Ketones at Room Temperature with Hydrogen Balloon. Advanced Synthesis and Catalysis, 2007, 349, 2039-2047.	4.3	94
197	Platinized mesoporous tungsten carbide for electrochemical methanol oxidation. Electrochemistry Communications, 2007, 9, 2576-2579.	4.7	122
198	CdS–AgGaS2 photocatalytic diodes for hydrogen production from aqueous Na2S/Na2SO3 electrolyte solution under visible light (λ≥420nm). Catalysis Today, 2007, 120, 174-181.	4.4	70

#	Article	IF	CITATIONS
199	Optimization of CdS/TiO2 nano-bulk composite photocatalysts for hydrogen production from Na2S/Na2SO3 aqueous electrolyte solution under visible light (λ≥420nm). Journal of Photochemistry and Photobiology A: Chemistry, 2007, 188, 112-119.	3.9	188
200	Photocatalytic hydrogen production from natural seawater. Journal of Photochemistry and Photobiology A: Chemistry, 2007, 189, 141-144.	3.9	117
201	Photocatalytic Ohmic layered nanocomposite for efficient utilization of visible light photons. Applied Physics Letters, 2006, 89, 064103.	3.3	66
202	Anoxic Hydrogen Production over CdS-based Composite Photocataiysts under Visible Light Irradiation (λ,≥420nm). Studies in Surface Science and Catalysis, 2006, , 201-204.	1.5	2
203	Fabrication of CdS/TiO2 nano-bulk composite photocatalysts for hydrogen production from aqueous H2S solution under visible light. Chemical Physics Letters, 2006, 425, 278-282.	2.6	168
204	Nanocomposite membranes of surface-sulfonated titanate and Nafion® for direct methanol fuel cells. Journal of Power Sources, 2006, 159, 1015-1024.	7.8	83
205	Montmorillonite functionalized with perfluorinated sulfonic acid for proton-conducting organic–inorganic composite membranes. Journal of Power Sources, 2006, 162, 180-185.	7.8	60
206	A Composite Photocatalyst of CdS Nanoparticles Deposited on TiO2 Nanosheets. Journal of Nanoscience and Nanotechnology, 2006, 6, 3642-3646.	0.9	42
207	Tungsten Carbide Microspheres as a Noble-Metal-Economic Electrocatalyst for Methanol Oxidation. Angewandte Chemie - International Edition, 2005, 44, 6557-6560.	13.8	257
208	Tungsten Carbide Microspheres as a Noble-Metal-Economic Electrocatalyst for Methanol Oxidation ChemInform, 2005, 36, no.	0.0	0
209	Voxel-based statistical analysis of cerebral glucose metabolism in the rat cortical deafness model by 3D reconstruction of brain from autoradiographic images. European Journal of Nuclear Medicine and Molecular Imaging, 2005, 32, 696-701.	6.4	29
210	Highly Efficient Overall Water Splitting Through Optimization of Preparation and Operation Conditions of Layered Perovskite Photocatalysts. Topics in Catalysis, 2005, 35, 295-303.	2.8	125
211	Photocatalytic Water Splitting Under Visible Light with Particulate Semiconductor Catalysts. Catalysis Surveys From Asia, 2005, 9, 217-227.	2.6	187
212	Development of Korean Standard Brain Templates. Journal of Korean Medical Science, 2005, 20, 483.	2.5	65
213	Synthesis of Nitrogen-Doped Titanium Oxide Nanostructures Via a Surfactant-Free Hydrothermal Route. Journal of Materials Research, 2005, 20, 3011-3020.	2.6	22
214	Photocatalytic Hydrogen Production from Water over M-Doped La2Ti2O7(M = Cr, Fe) under Visible Light Irradiation (λ > 420 nm)â€. Journal of Physical Chemistry B, 2005, 109, 2093-2102.	2.6	237
215	Photocatalytic hydrogen production from water–methanol mixtures using N-doped Sr2Nb2O7under visible light irradiation: effects of catalyst structure. Physical Chemistry Chemical Physics, 2005, 7, 1315-1321.	2.8	104
216	Nafion/Sulfonated Montmorillonite Composite:Â A New Concept Electrolyte Membrane for Direct Methanol Fuel Cells. Chemistry of Materials, 2005, 17, 1691-1697.	6.7	286

#	Article	IF	CITATIONS
217	Formation of La2Ti2O7 crystals from amorphous La2O3-TiO2 powders synthesized by the polymerized complex method. Korean Journal of Chemical Engineering, 2004, 21, 970-975.	2.7	9
218	Effects of Transition Metal Addition on the Solid-State Transformation of Molybdenum Trioxide to Molybdenum Carbides. Chemistry of Materials, 2004, 16, 307-314.	6.7	66
219	An Undoped, Single-Phase Oxide Photocatalyst Working under Visible Light. Journal of the American Chemical Society, 2004, 126, 8912-8913.	13.7	536
220	Neural changes associated with speech learning in deaf children following cochlear implantation. NeuroImage, 2004, 22, 1173-1181.	4.2	33
221	Age-associated changes of cerebral glucose metabolic activity in both male and female deaf children: parametric analysis using objective volume of interest and voxel-based mapping. NeuroImage, 2004, 22, 1543-1553.	4.2	27
222	The Preparation and Characterisation of Pd–ZnO Catalysts for Methanol Synthesis. Topics in Catalysis, 2003, 22, 319-324.	2.8	59
223	Effect of Zr Substitution for Ti in KLaTiO4 for Photocatalytic Water Splitting. Catalysis Letters, 2003, 90, 39-43.	2.6	48
224	Photocatalytic Water Splitting over La ₂ Ti ₂ O ₇ Synthesized by the Polymerizable Complex Method. Catalysis Letters, 2003, 91, 193-198.	2.6	112
225	Photocatalytic water splitting over ZrO2 prepared by precipitation method. Korean Journal of Chemical Engineering, 2003, 20, 1026-1029.	2.7	46
226	Electronic Band Structure and Photocatalytic Activity of Ln2Ti2O7 (Ln = La, Pr, Nd). Journal of Physical Chemistry B, 2003, 107, 4963-4970.	2.6	207
227	Photocatalytic Degradation of CH3Cl over a Nickel-Loaded Layered Perovskite. Industrial & Engineering Chemistry Research, 2003, 42, 1184-1189.	3.7	54
228	Nickel-loaded La2Ti2O7 as a bifunctional photocatalyst. Chemical Communications, 2002, , 2488-2489.	4.1	69
229	Comparison of polycarbonate precursors synthesized from catalytic reactions of bisphenol-A with diphenyl carbonate, dimethyl carbonate, or carbon monoxide. Journal of Applied Polymer Science, 2002, 86, 937-947.	2.6	28
230	Mn-Promoted Ni/Al2O3 Catalysts for Stable Carbon Dioxide Reforming of Methane. Journal of Catalysis, 2002, 209, 6-15.	6.2	124
231	In situ XAFS Characterization of Supported Homogeneous Catalysts. Topics in Catalysis, 2002, 18, 67-72.	2.8	13
232	Mg-Doped WO3 as a Novel Photocatalyst for Visible Light-Induced Water Splitting. Catalysis Letters, 2002, 80, 53-57.	2.6	186
233	Reply to Comment on "Quantitative Analysis of Tiâ~Oâ~'Si and Tiâ^'Oâ^'Ti Bonds in Tiâ^'Si Binary Oxides by the Linear Combination of XANES― Journal of Physical Chemistry B, 2001, 105, 6274-6274.	2.6	1
234	The role of MnO in Ni/MnO-Al2O3 catalysts for carbon dioxide reforming of methane. Applied Catalysis A: General, 2001, 215, 31-38.	4.3	74

#	Article	IF	CITATIONS
235	Cross-modal plasticity and cochlear implants. Nature, 2001, 409, 149-150.	27.8	575
236	Effects of Pretreatment Conditions on CO Oxidation over Supported Au Catalysts. Journal of Catalysis, 1999, 186, 1-11.	6.2	392
237	Stable carbon dioxide reforming of methane over modified Ni/Al2O3 catalysts. Catalysis Letters, 1998, 52, 43-47.	2.6	118
238	Molybdenum Nitride and Carbide Prepared from Heteropolyacid. Journal of Catalysis, 1998, 178, 119-136.	6.2	38
239	Effects of Copper Phase on CO Oxidation over Supported Wacker-Type Catalysts. Journal of Catalysis, 1998, 180, 123-131.	6.2	53
240	Thermal and chemical stability of titanium-substituted MCM-41. Catalysis Letters, 1996, 40, 261-264.	2.6	39
241	XAFS characterization of supported PdCl2â^'CuCl2 catalysts for CO oxidation. Reaction Kinetics and Catalysis Letters, 1996, 57, 227-236.	0.6	17
242	Effects of catalyst composition on methanol synthesis from CO2/H2. Korean Journal of Chemical Engineering, 1995, 12, 460-465.	2.7	17
243	Supported PdCl2î—, CuCl2 catalysts for carbon monoxide oxidation 1. Effects of catalyst composition and reaction conditions. Applied Catalysis B: Environmental, 1994, 5, 103-115.	20.2	41
244	In situ carburization of metallic molybdenum during catalytic reactions of carbon-containing gases. Catalysis Letters, 1993, 20, 97-106.	2.6	50